

HST and VLT observations of Isolated Neutron Stars

R. P. Mignani¹, G. G. Pavlov², A. De Luca³ and P. A. Caraveo⁴

¹*European Southern Observatory, Karl-Schwarzschild-Str. 2, D85740, Garching, Germany*

²*Pennsylvania State University, 525 Davey Lab, University Park, PA 16802, USA*

³*Istituto di Astrofisica Spaziale e Fisica Cosmica, Sezione di Milano "G.Occhialini" - CNR v. Bassini 15, I-20133 Milan, Italy*

⁴*Istituto di Astrofisica Spaziale e Fisica Cosmica, Sezione di Milano "G.Occhialini" - CNR v. Bassini 15, I-20133 Milan, Italy*

ABSTRACT

New results of HST and VLT observations of isolated pulsars and their environments are presented. We present the first deep optical observations of the nearby pulsar PSR J0108-1431, the identification evidence of PSR 1929+10 based on the proper motion measurement of its optical counterpart and a deep investigation at optical wavelengths of the X-ray PWN around Vela.

PSR J0108-1431

PSR J0108-1431 was discovered by Tauris et al. (1994) during the Parkes Southern Pulsar Survey. With a period $P = 0.808$ s and a period derivative $\dot{P} = 7.44 \times 10^{-17}$ s s⁻¹ (D'Amico et al. 1998), the pulsar has a characteristic age $P/2\dot{P} = 170$ Myr, rotation energy loss rate $\dot{E} = 5.6 \times 10^{30}$ erg s⁻¹, and magnetic field $B = 2.5 \times 10^{11}$ G. From the Taylor & Cordes model (1993), the low dispersion measure (2.38 ± 0.01 cm⁻³ pc) puts PSR J0108-1431 at a distance of 60-130 pc. Although very close, PSR J0108-1431 has never been detected so far outside the radio band. Virtually undetectable according to standard cooling models, which predict a temperature $T < 10^4$ K for an age of ~ 170 Myr (Tsuruta 1998), the detection of optical-UV thermal radiation from the neutron star (NS) surface would allow one to constrain possible heating mechanisms like the dissipation of energy of differential rotation (e.g. Van Riper et al. 1994) and Joule heating caused by dissipation of the magnetic field in the NS crust (Miralles, Urpin & Konenkov 1998). Thus, if some heating mechanisms indeed operate, one can expect the surface NS temperature of a few times 10^4 K, detectable in the optical-UV but undetectable in X-rays. Optical observations of PSR J0108-1431 were carried out with the 6-m telescope of Special Astrophysical Observatory (Russia), but they were not deep enough to detect the pulsar (Kurt et al. 2000). Therefore, we performed a deep observation with the Antu unit of the ESO Very Large Telescopes (VLT) between July and August 2000. Images were obtained in the Bessel filters U (9000s), B (5400s), and V (7200s) using the FOCAL Reducer and Spectrograph 1 (FORS1) instrument operated at its standard angular resolution of 0.2" per pixel, with a corresponding field of view of $6.8' \times 6.8'$. See Mignani, Manchester and Pavlov (2003) for details on the observations and the data reduction. To obtain an updated reference radio position of the pulsar, we performed new observations with the Australia Telescope Compact Array (ATCA) on 2001 March 31 in two bands centered on 1384 MHz and 2496 MHz. We derived a mean position (epoch 2001.3) of $\alpha_{J2000} = 01\ 08\ 08.317 \pm 0.010$ s, $\delta_{J2000} = -14\ 31\ 49.35 \pm 0.35''$, coincident within the uncertainties with that obtained from the timing data (D'Amico et al. 1998). This implies an upper limit on the pulsar proper motion of 82 mas yr⁻¹, corresponding to a total velocity $v < 50d_{130}$ km s⁻¹ (with d_{130} being the pulsar distance in units of 130 pc) i.e. within the bottom 10% of the measured pulsar velocity distribution (Lorimer, Bailes and Harrison 1997). By using as a reference the positions of stars selected from the GSC II, the most recent pulsar position was finally

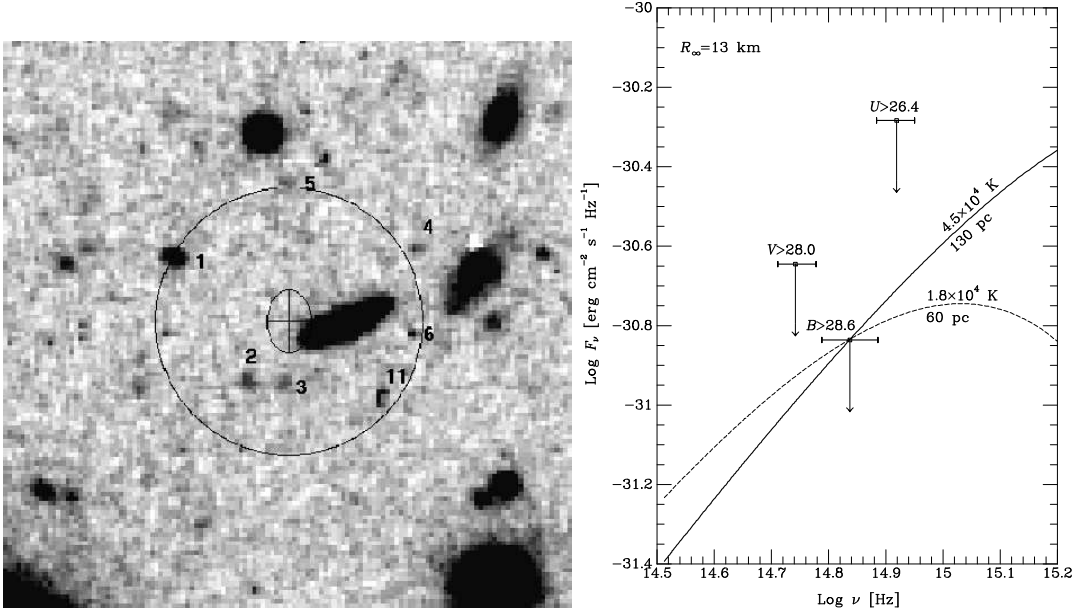


Fig. 1. (left) FORS1 $25'' \times 25''$ V-band image (7200s) of the PSR J0108–1431 field (North to the top, East to the left). The cross marks the nominal radio position of the pulsar, with the arms equal to 3 times the overall uncertainty on the pulsar position. Point-like objects detected at $\geq 3\sigma$ in at least one passband and located within (close to) a $\sim 6''$ radius around the pulsar position are labelled. (right) Upper limits on the pulsar fluxes in the UBV bands and blackbody spectra corresponding to the most stringent B -band limit for the distances of 60 and 130 pc and a neutron star radius $R_\infty = 13$ km.

registered on the FORS1 images (overall accuracy $0.33''$ in R.A. and $0.46''$ in Dec). The pulsar position at the epoch of our optical observations is marked in Fig.1 (left). To facilitate the object detection, all the images have been smoothed using a gaussian filter. The pulsar position falls about $\approx 0.6''$ East from an elliptical galaxy in the field. Since such a distance corresponds to about twice the uncertainty of the pulsar position in R.A, it is unlikely that the pulsar is hidden behind the galaxy, but we cannot rule it out. Only few point-like objects (labelled in Fig.1, left) have been detected within a radius of $6''$ from the pulsar position but they are too distant from the nominal pulsar position to be considered candidate counterparts. Therefore, we conclude that no optical counterpart to the pulsar can be identified in our data down to 3σ upper limits of $V \simeq 28$, $B \simeq 28.6$ and $U \simeq 26.4$ e.g. more than 3 magnitudes deeper than those obtained by Kurt et al. (2000). For a distance of 130 pc, estimated from the pulsar's dispersion measure, our constraints on the optical flux put an upper limit of $T = 4.5 \times 10^4$ K for the surface temperature of the neutron star, assuming a stellar radius $R_\infty = 13$ km.

PSR B1929+10

PSR1929+10 is also an old ($\sim 3 \times 10^6$ yrs) and relatively nearby (~ 330 pc - Brisen et al. 2002) radio pulsar. Originally detected in X-ray with Einstein (Helfand 1983), pulsations at the radio period (227 ms) were discovered by ROSAT (Yancopulous et al. 1994) and confirmed by ASCA (Wang and Halpern 1997). The X-ray spectrum could be either thermal ($T \sim 3-5 \times 10^6$ K) and produced from hot polar caps (Yancopulous et al. 1994; Wang and Halpern 1997) or non-thermal with a spectral index $\alpha \approx 1.27 \pm 0.4$ (Becker and Trümper 1997). A candidate optical counterpart was identified with the HST/FOC by Pavlov et al. (1996) from the positional coincidence with the radio coordinates. To secure the identification of the PSR B1929+10 optical counterpart we have applied the strategy used by Mignani et al.(2000), i.e., the measure of a proper motion consistent with the radio one. The field of PSR B1929+10 was imaged with the HST/STIS between August and October 2001. Ten 1200s exposures were obtained over five visits with the NUV-MAMA detector ($24.7' \times 24.7'$ field of view, $0.024''$ pixel size) through the F25QTZ filter ($\lambda = 2364\text{\AA}$, $\Delta\lambda \sim 842\text{\AA}$ FWHM). The STIS time-integrated images were calibrated using the standard HST pipeline and corrected for the CCD

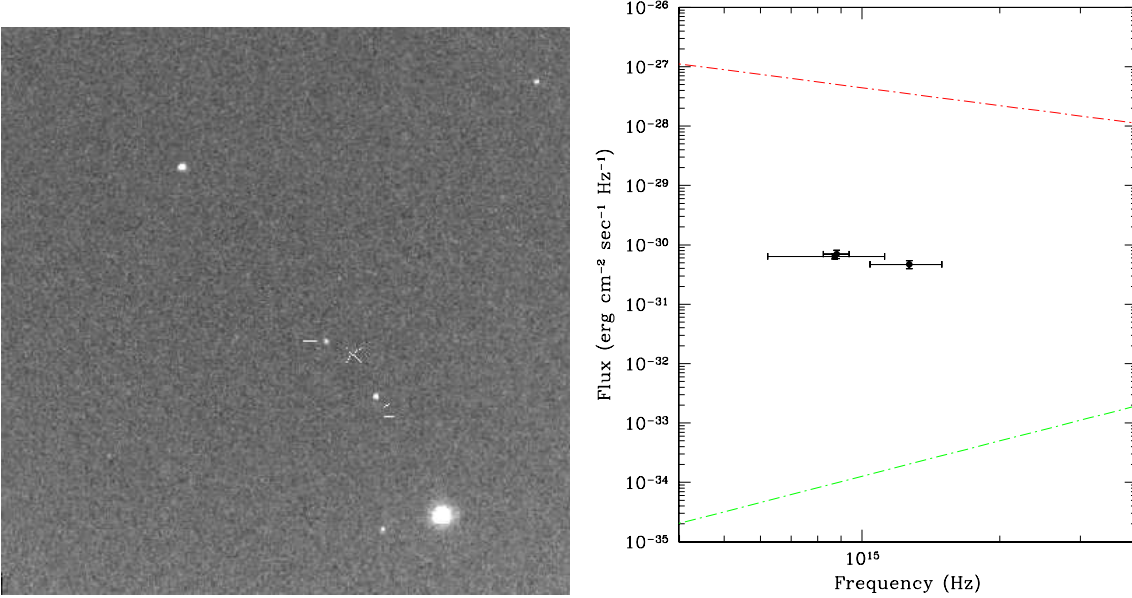


Fig. 2. (left) STIS/NUV-MAMA/F25QTZ image of the PSR 1929+10 field (12000S). North to the top, East to the left. The pulsar candidate counterpart is marked by the two ticks. The cross marks the position of the pulsar at epoch 1994.52. (right) Multiband optical flux distribution of PSR 1929+10 from the photometry of Mignani et al. (2002) and (Pavlov et al. 1996). The two dashed lines represents the optical extrapolation of the best fitting X-ray spectral models.

geometric distortion. As starting point for our proper motion measurement we used the FOC observations of Pavlov et al. (1996), retrieved from the ST-ECF public archive and recalibrated on-the-fly. A complete description of the relative astrometry procedure with a detailed discussion of the error budget is reported in Mignani et al.(2002). After the registration of the different epoch images in a unique reference frame, we could measure the candidate optical counterpart displacement over the 7.2 years (Fig.2, left). The five independent measurements yielded results fully consistent within the errors. By means of a simple χ^2 fit we obtained the best proper motion values: $\mu_\alpha \cos(\delta) = +97 \pm 1$ mas yr $^{-1}$ $\mu_\delta = +46 \pm 1$ mas yr $^{-1}$ corresponding to a position angle (PA) of $64.63^\circ \pm 0.55^\circ$. Within the errors, these results are fully compatible in both magnitude and direction with the radio ones (Briskin et al. 2002): $\mu_\alpha \cos(\delta) = +94.82 \pm 0.26$ mas yr $^{-1}$ $\mu_\delta = +43.04 \pm 0.15$ mas yr $^{-1}$ (PA= $65.58^\circ \pm 0.09^\circ$). Our proper motion measurement thus provide a robust proof that the candidate proposed by Pavlov et al.(1996) is indeed the optical counterpart of PSR B1929+10. The STIS/F25QTZ flux of the pulsar has been compared with the photometry of Pavlov et al. (1996) in the F130LP ($\lambda = 3437.7\text{\AA}$, $\Delta\lambda \sim 1965\text{\AA}$ FWHM) and F342W ($\lambda = 3402\text{\AA}$, $\Delta\lambda \sim 442\text{\AA}$ FWHM) filters. At a variance with middle-aged ($\sim 10^5$ yrs) pulsars such as PSR B0656+14, PSR B1055-52 and Geminga, for which the optical fluxes are somewhat compatible with the extrapolations of their X-ray spectra, the flux of the PSR 1929+10 candidate counterpart deviates by about 3 orders of magnitude from the predicted values (Fig.2, right). In addition, the data seems to be consistent with a power law, with spectral index $\alpha = 0 \div 1$, depending on the actual value of the reddening. This result is apparently in contrast with the available data from young to middle-aged pulsars which suggest, as a general trend, a decreasing importance of non-thermal processes with the age.

The Vela pulsar optical nebula

A compact ($\sim 4'$) X-ray nebula around the Vela pulsar was detected in soft X-rays with the *Einstein* HRI (Harnden et al. 1985) and firstly interpreted as a pulsar-wind nebula (PWN) powered by relativistic particles ejected by the pulsar, which shock in the ambient medium and emit synchrotron radiation. Based on its “kidney-bean” shape, Markwardt & Ögelman (1998) proposed an interpretation in terms of a bow-shock produced by the supersonic motion of the pulsar through the ambient medium. The Vela pulsar and its

PWN have been recently observed with both the High Resolution Camera (HRC) and the Advanced CCD Imaging Spectrometer (ACIS) on board the *Chandra* X-ray observatory. Thanks to the excellent angular resolution of *Chandra*, the morphology of the PWN was resolved in a complex structure, similar to that of the Crab PWN, which cannot be explained by a simple bow-shock model. The brighter part of the PWN ($\approx 2'$), shows an approximately axisymmetric structure, with two arcs, a jet, and a counter-jet, embedded into an extended diffuse emission. The axis of symmetry, which can be associated with the pulsar rotational axis, nearly coincides with the direction of the pulsar's proper motion (P.A. = 301° — e.g., Caraveo et al. 2001a). The inner PWN is then surrounded by a bean-shaped diffuse nebula ($\sim 2' \times 2'$) with an elongated region of fainter diffuse emission southwest of the brighter part of the PWN and detected up to $\sim 4'$ from the pulsar. A $100''$ -long outer jet is also seen northwest of the inner PWN. The overall spectrum of the PWN can be described by a power law with an average spectral (energy) index $\alpha \approx 0.5$, which can be interpreted as synchrotron emission of relativistic electrons and/or positrons. Such a spectrum is expected to extend to optical and radio frequencies. Although the radio emission from the compact nebula is probably dominated by the brightness of the pulsar, highly polarized (up to 60% at 5 GHz) extended ($\sim 4'$) radio emission has been indeed detected in the surrounding region (Lewis et al. 2002; R. Dodson 2002, private communication) with two radio lobes southeast ($\sim 18 \text{ arcmin}^2$) and northeast ($\sim 5 \text{ arcmin}^2$) wrt the pulsar. One can then expect the presence of an optical nebula around the Vela pulsar, as observed in several other young pulsars like the Crab PWN (see, e.g., Hester et al. 2002, and references therein) and PSR B0540–69 (Caraveo et al. 2001b). Contrary to the Crab and PSR 0540-69, searches for the Vela PWN in optical have been inconclusive so far. Ögelman et al. (1989) reported only a marginal detection of a putative optical PWN ($\sim 2'$).

Tel.	Instr.	FOV	Scale	Date	Filter	λ ($\Delta\lambda$)	Exp. (s)
NTT	EMMI-B	$6.2' \times 6.2'$	$0.37''$	Jan 1995	<i>U</i>	3542\AA (542\AA)	4800
	EMMI-B	$6.2' \times 6.2'$	$0.37''$	Jan 1995	<i>B</i>	4223\AA (941\AA)	1800
	EMMI-R	$9.2' \times 8.6'$	$0.27''$	Jan 1995	<i>V</i>	5426\AA (1044\AA)	1200
	EMMI-R	$9.2' \times 8.6'$	$0.27''$	Jan 1995	<i>R</i>	6410\AA (1540\AA)	900
<i>HST</i>	WFPC2	$2.6' \times 2.6'$	$0.1''$	Jun 1997	555W	5500\AA (1200\AA)	2600
	WFPC2	$2.6' \times 2.6'$	$0.1''$	Jan 1998	555W	-	2000
	WFPC2	$2.6' \times 2.6'$	$0.1''$	Jun 1999	555W	-	2000
	WFPC2	$2.6' \times 2.6'$	$0.1''$	Jan 2000	555W	-	2600
	WFPC2	$2.6' \times 2.6'$	$0.1''$	Jul 2000	555W	-	2600
	WFPC2	$2.6' \times 2.6'$	$0.1''$	Mar 2000	675W	6717\AA (1536\AA)	2600
	WFPC2	$2.6' \times 2.6'$	$0.1''$	Mar 2000	814W	7995\AA (1292\AA)	2600
<i>VLT</i>	FORS1	$6.8' \times 6.8'$	$0.2''$	Apr 1999	<i>R</i>	6750\AA (1500\AA)	300
	FORS1	$6.8' \times 6.8'$	$0.2''$	Apr 1999	<i>I</i>	7680\AA (1380\AA)	300
ESO/MPG 2.2m	WFI	$34' \times 33'$	$0.24''$	Apr 1999	H_α	6588\AA (74.3\AA)	3600

Table 1. Available optical datasets for the Vela pulsar field. The first four columns list the telescope and the detector used for the observations, the field of view and the pixel scale, respectively. The epoch of observation is in column five. The filter names are listed in column six, with their pivot wavelengths and widths in column seven. The total integration time per observation (in seconds) is given in column eight.

Here we discuss the results of spatial correlations between the recently obtained *Chandra* ACIS images and *HST* WFPC2 images, together with observations obtained with the ESO *NTT/VLT/2.2m* telescopes (Mignani et al. 2003). See Table 1 for a detailed summary of the optical observations. For a direct comparison, optical and X-ray images have been superimposed with respect to the absolute (α, δ) reference frame, relying on the astrometric solution of each image. The absolute frame registration between the optical and X-ray images turned out to be accurate within $\approx 1''$ – $2''$, comparable with the uncertainty in the absolute astrometry of each frame. Our starting point was the combined WFPC2 F555W image, which is by far the

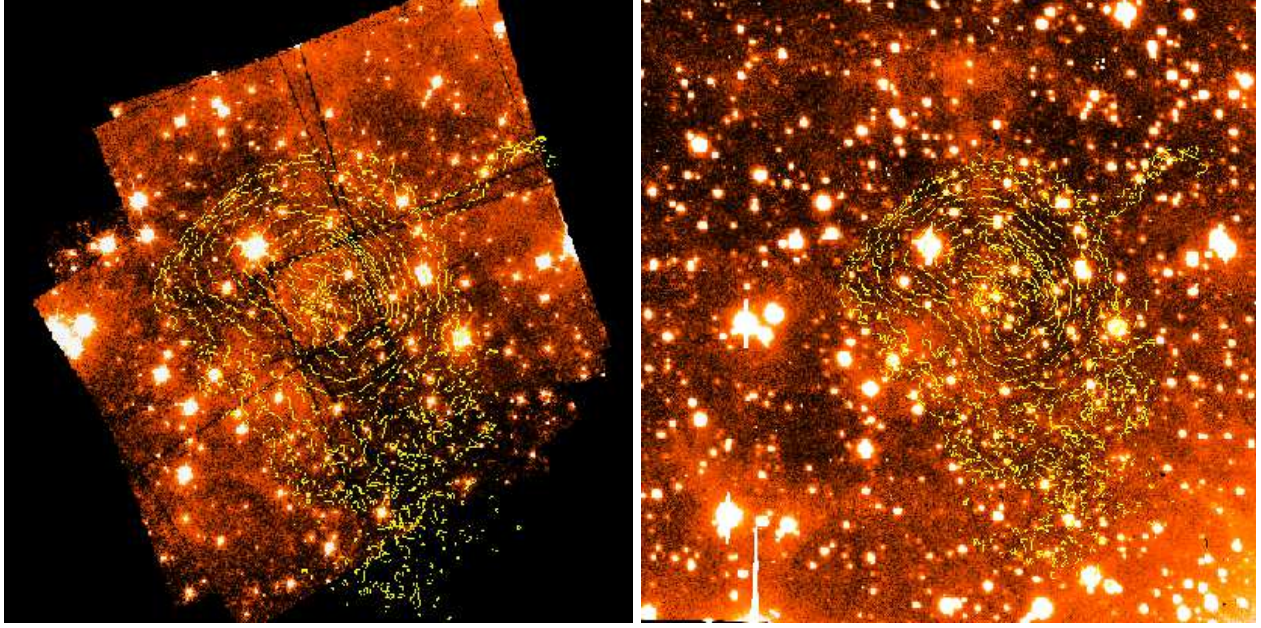


Fig. 3. (left) Combined WFPC2/555W image of the Vela pulsar field (11800s). North to the top, East to the left. The pulsar position is located within the innermost contour. (right) Combined *UBVR* image of the Vela pulsar field obtained from the *NTT*/EMMI observations. The overlaid contours (logarithmic scale) correspond to the X-ray intensity maps obtained from the *Chandra* ACIS image of the field integrated over the energy band (1–8 keV).

deepest optical image of the Vela pulsar field. The final image is shown in Fig. 3 (left), where we have superimposed the X-ray contour map obtained from the combined *Chandra* ACIS exposure of the region. The point source within the innermost X-ray contour is the optical counterpart of the Vela pulsar. The central PC field is large enough to map the inner part of the X-ray PWN, i.e., the inner arc, the jet and the counter-jet, easily identifiable in the contour map. Unfortunately, the outer arc region is partially coincident with the CCD gaps between the PC and WFC chips. No optical counterparts of the known X-ray features can be identified in the combined WFPC2/555W image, nor any other structure symmetric to the pulsar proper motion direction (Fig.3 - left). We set 3σ upper limits of $27.4 \text{ mag arcsec}^{-2}$ ($0.39 \times 10^{-30} \text{ ergs cm}^{-2} \text{ s}^{-1} \text{ Hz}^{-1} \text{ arcsec}^{-2}$) and $27.1 \text{ mag arcsec}^{-2}$ ($0.57 \times 10^{-30} \text{ ergs cm}^{-2} \text{ s}^{-1} \text{ Hz}^{-1} \text{ arcsec}^{-2}$) for the innermost region (inner arc, jet, and counter-jet) and the outer arc, respectively. After correcting for interstellar extinction, these values translate to $\approx 27.0 \text{ mag arcsec}^{-2}$ ($0.52 \times 10^{-30} \text{ ergs cm}^{-2} \text{ s}^{-1} \text{ Hz}^{-1} \text{ arcsec}^{-2}$) and $\approx 26.7 \text{ mag arcsec}^{-2}$ ($0.57 \times 10^{-30} \text{ ergs cm}^{-2} \text{ s}^{-1} \text{ Hz}^{-1} \text{ arcsec}^{-2}$), respectively. The analysis was repeated for the rest of the optical database, but no evidence for a compact optical nebula was found. We used the wider *NTT* images to search for diffuse optical emission up to distances of $\approx 3 \text{ arcmin}$, in particular at the position of the southwest extension of the X-ray nebula. Although many background enhancements can be recognized in the combined *NTT UBVR* image (Fig.3 - right), they can be also identified in the ESO/2.2m H_α one, suggesting that they are most likely associated with the bright filaments of the Vela supernova remnant. We thus put upper limits on the extended emission of $25.4 \text{ mag arcsec}^{-2}$ ($2.5 \times 10^{-30} \text{ ergs cm}^{-2} \text{ s}^{-1} \text{ Hz}^{-1} \text{ arcsec}^{-2}$). We have compared the measured optical upper limits on the brightness of the Vela PWN for the outer arc and the diffuse emission southwest of the pulsar with the extrapolation of the X-ray and radio data. While the optical upper limits for the inner/outer arcs are close to such extrapolation, in the case of the southwest diffuse emission they lie about 3 orders of magnitudes above the expected value (Mignani et al. 2003). To summarize, we conclude that it is very likely that just a slightly deeper optical observation would allow one to detect the outer/inner arc (and other bright elements of the inner PWN), while even deeper optical observations are needed to detect the emission from the Vela PWN at large.

REFERENCES

- Becker, W. and Trümper, The X-ray luminosity of rotation-powered neutron stars, *A&A* **326**, 682, 1997
- Briskin, W.F., Benson, J.M., Goss, W.M. and Thorsett, S.E., Very Long Baseline Array Measurement of Nine Pulsar Parallaxes, *ApJ* **571**, **906**, 2002
- Caraveo, P. A., De Luca A., Mignani R. P., & Bignami, G.F, The Distance to the Vela Pulsar Gauged with Hubble Space Telescope Parallax Observations, *ApJ* **561**, 930, 2001a
- Caraveo, P. A., Mignani, R. P., De Luca, A. et al., SNR0540-69-the Crab Twin-Revisited: Chandra vs. HST, in Proc. STScI Symp., A Decade of HST Science, eds. M. Livio, K. Noll, & M. Stiavelli, 105, 2001b
- D'Amico, N., Stappers, B. W., Bailes, M., et al., The Parkes Southern Pulsar Survey - III, *MNRAS* **297**, 28, 1998
- Harnden, F. R., Grant, P. D., Seward, F. D., & Kahn, S. M., Einstein observations of VELA X and the VELA pulsar, *ApJ* **299**, 828, 1985
- Hester, J. J., Mori, K., Burrows, D., et al., Hubble Space Telescope and Chandra Monitoring of the Crab Synchrotron Nebula, *ApJ* **577**, L49, 2002
- Helfand, D.J., X-rays from radio pulsars - The portable supernova remnants, in IAU Symp. 101, Supernova Remnants and Their X-ray Emissions, eds. J. Danziger and P. Gorenstein, 471, 1983
- Kurt, V. G., Komarova, V. N., Fatkhullin, T. A. et al., Photometric study of fields of nearby pulsars with the 6m telescope, *Bull. Special Astrophys. Obs.*, **49**, 5, 2000
- Lewis, D., Dodson, R., McConnell, D., & Deshpande, A., The Vela Pulsar Wind Nebula at 6 cm, in Neutron Stars in Supernova Remnants, ASP Conf. Ser., eds. P. O. Slane & B. M. Gaensler, **271**, 191, 2002
- Lorimer, D. R., Bailes, M., & Harrison, P. A., Pulsar statistics - IV, *MNRAS*, **289**, 592, 2002
- Markwardt, C. B. & Ögelman, H. B., The X-ray bow shock nebula of the Vela pulsar, *MSAIt* **69**, 927, 1998
- the Discovery, *Frontiers science series* Eds. N. Shibazaki et al., **24**, 335, , 1998
- Mignani, R.P., Manchester, R.N., Pavlov, G.G., Search for the optical counterpart of the nearby pulsar J0108-1431, *ApJ* - in press, 2002
- Mignani, R.P., De Luca, A., Caraveo, P.A., The Hubble Space Telescope Revisits the Proper Motion of Pulsar B0656+14, *ApJ* **543**, **318**, 2000
- Mignani, R.P., De Luca, A., Caraveo, P.A., Becker, W., HST Proper Motion confirms the optical identification of the nearby pulsar PSR 1929+10, *ApJ*, **580**, L147, 2002
- Mignani, R.P., De Luca, A., Kargaltsev, O. et al., Search for the optical counterpart of the Vela pulsar X-ray nebula, submitted to *ApJ*, 2002
- Miralles, J. A., Urpin, V., & Konenkov, D., Joule Heating and the Thermal Evolution of Old Neutron Stars, *ApJ* **503**, 368, 1998
- Ögelman, H. B, Koch-Miramond, L., & Aurie re, M., Measurement of the Vela pulsar's proper motion and detection of the optical counterpart of its compact X-ray nebula, *ApJ* **342**, L83, 1989
- Pavlov, G.G., Stringfellow, G.S. and C rdova, F.A., Hubble Space Telescope Observations of Isolated Pulsars, *ApJ* **467**, 370, 1996
- Pavlov, G. G., Zavlin, V. E., Sanwal, D. et al., The X-Ray Spectrum of the Vela Pulsar Resolved with the Chandra X-Ray Observatory, *ApJ* **552**, 129, 2001a
- Pavlov, G. G., Kargaltsev, O. Y., Sanwal, D., & Garmire, G. P., Variability of the Vela Pulsar Wind Nebula Observed with Chandra, *ApJ* **554**, L189, 2001b
- Tauris, T. M., Nicastro, L., Johnston, S. et al., Discovery of PSR J0108-1431: The closest known neutron star? *ApJ* **428**, L53, 1994
- Taylor, J. H., & Cordes, J. M., Pulsar distances and the galactic distribution of free electrons, *ApJ*, **411**, 674, 1993
- Tsuruta, S., Thermal properties and detectability of neutron stars II, *Phys. Rep.* **291**, 1, 1998
- Van Riper, K. A., Link, B., & Epstein, R. I., Frictional Heating and Neutron Star Thermal Evolution, *ApJ* **448**, 294, 1995
- Yancopoulos, A., Hamilton, T.T. and Helfand, D.J., The detection of pulsed X-ray emission from a nearby radio pulsar, *ApJ* **429**, 832, 1994
- Wang, F.Y.H. & Halpern, J.P., ASCA Observations of PSR 1929+10 and PSR 0950+08, *ApJ* **482**, L159, 1997

